Distribution pattern of mercury in northern Barents Sea and Eurasian Basin surface sediment

Stephen G Kohler, Laura M Kull, Lars-Eric Heimbürger-Boavida, Thaise Ricardo de Freitas, Nicolas Sanchez, Kuria Ndungu, Murat V Ardelan

Marine Pollution Bulletin 185 (2022) 114272

Contents lists available at ScienceDirect

Marine Pollution Bulletin

journal homepage: www.elsevier.com/locate/marpolbul

Baseline

Distribution pattern of mercury in northern Barents Sea and Eurasian Basin surface sediment

Stephen G. Kohler [a,*], Laura M. Kull [a], Lars-Eric Heimbürger-Boavida [b], Thaise Ricardo de Freitas [c], Nicolas Sanchez [a], Kuria Ndungu [d], Murat V. Ardelan [a,*]

[a] Department of Chemistry, Norwegian University of Science and Technology (NTNU), Høgskoleringen 5, NO-7491 Trondheim, Norway
[b] Aix-Marseille Université, CNRS/INSU, University de Toulon, IRD, Mediterranean Institute of Oceanography (MIO), Bât. Méditerranée, Campus de Luminy-Océanomed, 13009 Marseille, France
[c] Department of Geosciences, University of Oslo (UiO), Sem Sælands vei 1, 0371 Oslo, Norway
[d] Norwegian Institute for Water Research (NIVA), Økernveien 94, NO-0579 Oslo, Norway

ARTICLE INFO

Keywords:
Arctic
Barents Sea
Eurasian Basin
Mercury
Sediments

ABSTRACT

Marine sediment is a significant sink for the global pollutant mercury. In a rapidly changing Arctic region, mercury (Hg) bioaccumulation in the marine ecosystem remains a prominent environmental issue. Here, we report surface sediment (0–2 cm) concentrations of Hg and other toxic elements of interest (Cr, Ni, Zn, Cu, As, Cd, Pb) in the northern Barents Sea and Eurasian Basin. We observed average Hg concentrations of 65 ± 23 ng/g with the highest concentration of 116 ng/g in the Eurasian Basin. Our calculated enrichment factors suggest low anthropogenic enrichment for mercury, chromium, nickel, and copper. Mercury and trace element geographic patterns are best explained by the origin and transportation of fine grain sediment towards the Eurasian Basin, with scavenging by both particulate organic carbon and metal oxides as significant delivery mechanisms.

A warming global climate is driving elevated ocean temperatures, accelerated losses of sea ice, thawing permafrost, and an increased geopolitical interest in the Arctic Ocean. Consequently, these changes may have a negative impact on the vulnerable Arctic marine ecosystem. The ramifications of climate change will also impact the biogeochemical cycle of the global pollutant mercury (Chetélat et al., 2022; McKinney et al., 2022). Mercury (Hg) concentrations in Arctic biota are elevated despite an absence of important local anthropogenic sources. Thus, most of the Hg in the Arctic region comes from fossil fuel burning, mining, and other human-related activities in lower latitudes and transported to the general Arctic region via atmospheric transport (Dastoor et al., 2022). For the Arctic Ocean, Hg is delivered about equally via atmospheric deposition, the major pan-Arctic rivers, oceanic currents and erosion, along with minor inputs from snow and glacial melt (Dastoor et al. (2022) and references therein). Additionally, large stores of natural Hg in permafrost (Schuster et al., 2018) may be released in the future and shuttled to the Arctic shelves because of climate change.

Increased Hg inputs to the Arctic Ocean shelves suggest marine sediments will be the major sink for Hg in this area. Current Arctic Hg budgets may already underestimate sediment Hg burial by over 100 % (Dastoor et al., 2022), suggesting a substantial increase in total Hg delivered to marine sediments under climate change scenarios. Recent measurements of Hg isotopic signatures in Arctic fjord sediment cores historically suggest Hg delivery is modulated by climatic changes (Lee et al., 2021). The current rapid warming in the Arctic region indicates that glacial melt, rivers, and erosion will deliver more Hg to Arctic shelf surface waters. At the same time, the concurrent increase in primary production and particulate matter fluxes may deliver large amounts of Hg and organic matter (OM) of marine origin to the sediments, stimulating transformation to bioaccumulative methylmercury (MeHg) (Mazrui et al., 2016). Subsequent diffusion from Arctic shelf sediments represents a significant MeHg source to the Arctic Ocean (Kim et al., 2020), which could drive increased MeHg concentrations in Arctic biota. As the northern Barents Sea is poised to become the first Arctic shelf sea to transition to a warm and well-mixed Atlantic water shelf sea (Lind et al., 2018), baseline measurements of Hg and other contaminants in marine sediments are critical.

In the northern Barents Sea, a lack of major riverine sources suggests

* Corresponding author.
E-mail addresses: stephen.g.kohler@ntnu.no (S.G. Kohler), lauramk@stud.ntnu.no (L.M. Kull), lars-eric.heimburger@mio.osupytheas.fr (L.-E. Heimbürger-Boavida), t.r.de.freitas@geo.uio.no (T. Ricardo de Freitas), nicolas.sanchez@ntnu.no (N. Sanchez), Kuria.Ndungu@niva.no (K. Ndungu), murat.v.ardelan@ntnu.no (M.V. Ardelan).

https://doi.org/10.1016/j.marpolbul.2022.114272
Received 16 September 2022; Received in revised form 14 October 2022; Accepted 16 October 2022
Available online 30 October 2022

that the major Hg inputs to surface waters are atmospheric deposition, oceanic transport, and erosion from Svalbard, Franz Josef Land and Novaya Zemlya. In addition, snow and glacial melt supply organic carbon (OC) bound-Hg to fjords in the Svalbard archipelago (Kim et al., 2020), where scavenging within the water column by particulate matter delivers Hg to marine sediments (Tesán et al., 2020). On the Arctic shelves, studies have suggested that increases in primary production, type of OM, hydrodynamic sorting, and diagenesis are all controlling factors explaining sedimentary distributions of Hg and other trace elements (Aksentov et al., 2021; Gobeil et al., 1999; Li et al., 2021; Liem-Nguyen et al., 2022; Ye et al., 2019). In sediment cores, elevated enrichment factors (EF) of bulk Hg in the surface have also been attributed to recent anthropogenic inputs in Greenland (Asmund and Nielsen, 2000), the Laptev and East Siberian Seas (Aksentov et al., 2021), and the southern Barents Sea (Everaert et al., 2017). However, knowledge of Hg and other toxic elements in marine sediments in the central Arctic Basin and the rapidly changing northern Barents Sea remains poor.

In this study, we measured bulk concentrations of Hg and other trace elements in surface sediments of the northern Barents Sea and Eurasian Basin. We evaluate EFs and sediment quality status of Hg and other trace elements, explore sediment distribution patterns of Hg, and discuss its influencing factors.

The sampling locations in the northwestern Barents Sea and Eurasian Basin were sampled on five cruises on *R/V Kronprins Haakon* as part of The Nansen Legacy project between August 2019 and September 2021 (Fig. 1). Samples in the northeastern Barents Sea were collected on *R/V Dalniye Zelentsy* in October and November 2019. All samples were collected either via box corer or Van Veen grab. Sediment was collected from the upper 0–2 cm and subsampled into trace-metal free tubes (Falcon) while avoiding all contact with metal equipment. Samples were subsequently frozen on board at −20 °C until further processing. In the laboratory, samples were freeze-dried and then homogenized using a trace-metal clean non-metallic mortar and pestle (polyetheretherketone).

Sediment samples were measured for total Hg by atomic absorption via thermal decomposition using a Direct Mercury Analyzer (DMA-80, Milestone). Selected samples were analyzed in duplicate and triplicate. The DMA was calibrated each use with a five-point calibration curve using the BrooksRand $HgCl_2$ standard (1.0 ± 0.006 mg/L) traceable to NIST 1641E. Accuracy and precision of the method were determined using two reference materials, marine sediment MESS-4 (n = 56) and estuarine sediment BCR-277R (n = 3). Recoveries of both reference materials were within the 95 % confidence interval with RSDs <5 % (Supplementary Data Table 1). Measurements from the same stations that were sampled during several cruises were averaged together if they were within 15 km^2 for plotting and statistical analysis. Additionally, approximately 250 mg of dried homogenized sediment sample was digested in a 50 % v/v clean HNO_3 acid mixture using an Ultraclave

Table 1
Regional data of Hg concentrations in surface sediments of the Arctic Ocean.

Location	Average Hg (ng/g)	Range Hg (ng/g)	Source
Northern Barents Sea	55	21–94	This study
Southern Barents Sea	36	16–63	Knies et al., 2008
Barents Sea	58		Novikov, 2017
Outer shelf		38–98	Tesán et al., 2020
Laptev Sea	51	30–96	Liem-Nguyen et al., 2022
East Siberian Sea	74	55–97	Kim et al., 2020
East Siberian Sea	36	13–92	Aksentov et al., 2021
Chukchi Sea	31	5–55	Fox et al., 2014
Chukchi Sea	32	9–78	Sattarova et al., 2022
Eurasian Basin	87	63–116	This study
Arctic Basin	~77	57–116	Gobeil et al., 1999
Arctic Basin		36–145	Tesán et al., 2020

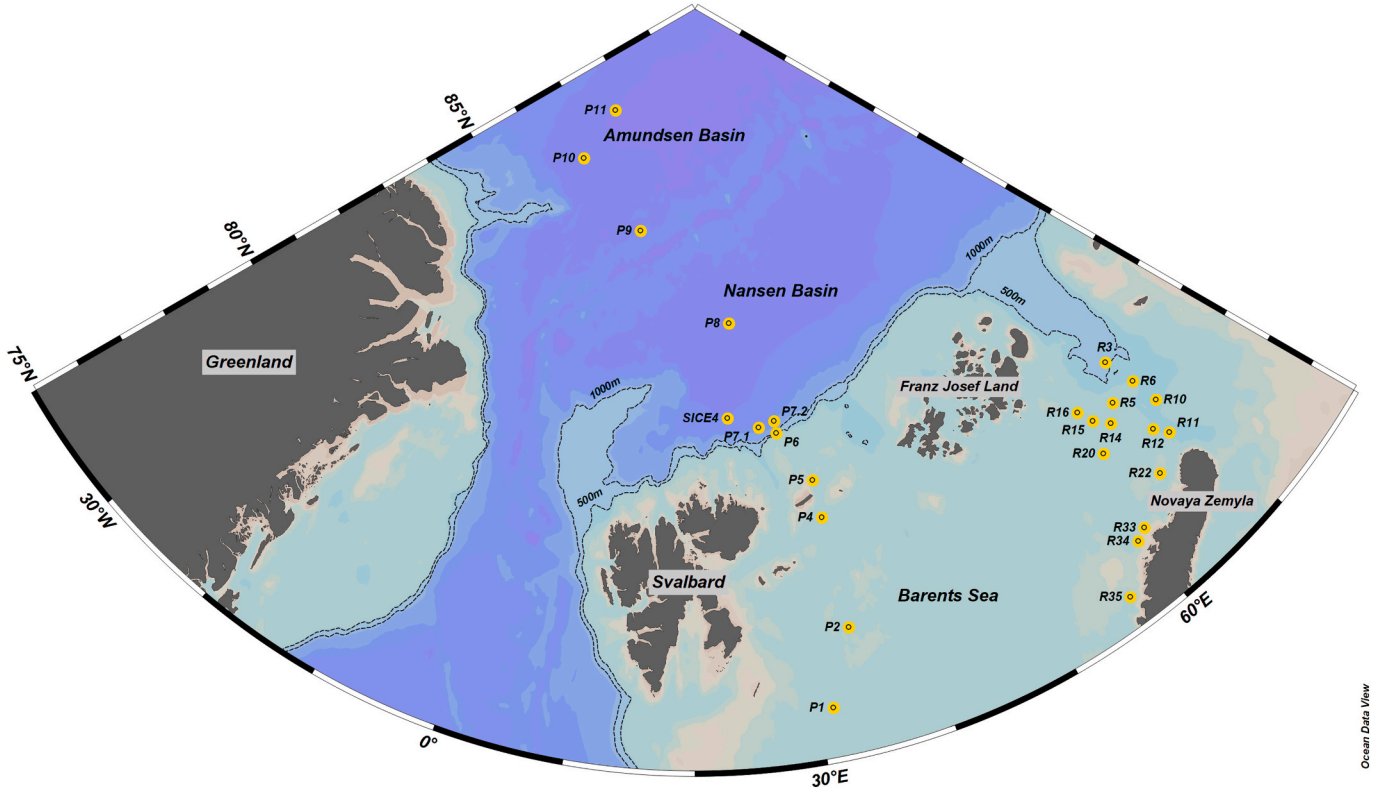

Fig. 1. Map of sampling stations in the Barents Sea and Eurasian Basin. Map created with Ocean Data View.

(Milestone). Samples were analyzed for Al, Fe, and trace elements (Li, V, Cr, Mn, Co, Ni, Cu, Zn, As, Ag, Cd, Pb) on an 8800 triple quadrupole ICP-MS (Agilent Technologies) using O_2 or H_2 as a reaction gas in MS/MS mode, depending on the element. Accuracy and precision of the method were determined using the certified reference materials MESS-4 ($n = 3$) and BCR-277R ($n = 3$), with all recoveries between 82 and 107 % (Supplementary Data Table 1). All metal concentrations are reported in dry weight.

Samples were analyzed for OM content using the loss-on-ignition (LOI) technique (Heiri et al., 2001) and for total organic carbon content (TOC %) using the DIN19539 method using a Primacs SNC100 Total Organic Carbon analyzer. Samples analyzed in triplicate for LOI had RSDs <5 % and samples analyzed in duplicate and triplicate for TOC % had RSDs <2 %.

To evaluate potential contamination from anthropogenic sources, EFs were calculated for surface sediments for environmental metals of interest Cr, Ni, Cu, Zn, As, Cd, Hg, and Pb using the following equation:

$$EF = [(El_s)/(Li_s)]/[(El_b)/(Li_b)]$$

El is the element of interest in surface sediment (s), normalized to lithium (Li_s) in surface sediment (Loring, 1990). This ratio is compared to background (b) dry weight concentrations of both El and Li. As the best way to evaluate enrichment factors is to use background data from the specific survey area (Abrahim and Parker, 2008), background concentrations for all elements of interest were assessed by evaluating sediment core data from the MAREANO project in the Barents Sea (Jensen et al., 2022). The elemental ratio El_b/Li_b from the 10 cm core depth interval was averaged for 13 selected sediment cores above the 74°N latitude line chosen from the MAREANO dataset. Based on sedimentation rate data from this shelf region, 0.7 ± 0.4 mm/yr (Zaborska et al., 2008), the 10 cm depth interval represents an approximate pre-industrial period of ~1850–1900. An EF > 1.0 in surface sediments suggests enrichment compared to the background value and could indicate potential anthropogenic input.

Maps were created with the publicly available Ocean Data View (Schlitzer, 2021) using weighted-average gridding. Statistical processing was performed in SPSS software to evaluate Pearson correlations and *Z*-score normalization with Varimax rotation for principal component analysis (PCA). Two principal components (PC) were extracted. The viability of a PCA plot was assessed using the Kaiser-Meyer-Olkin Measure for sampling adequacy and Bartlett's test for sphericity.

Total Hg concentrations in all surface sediment samples (Fig. 2A) ranged from 21 to 116 ng/g and were on average 65 ± 23 ng/g (1SD). Our observed Hg concentrations are within the range to those previously

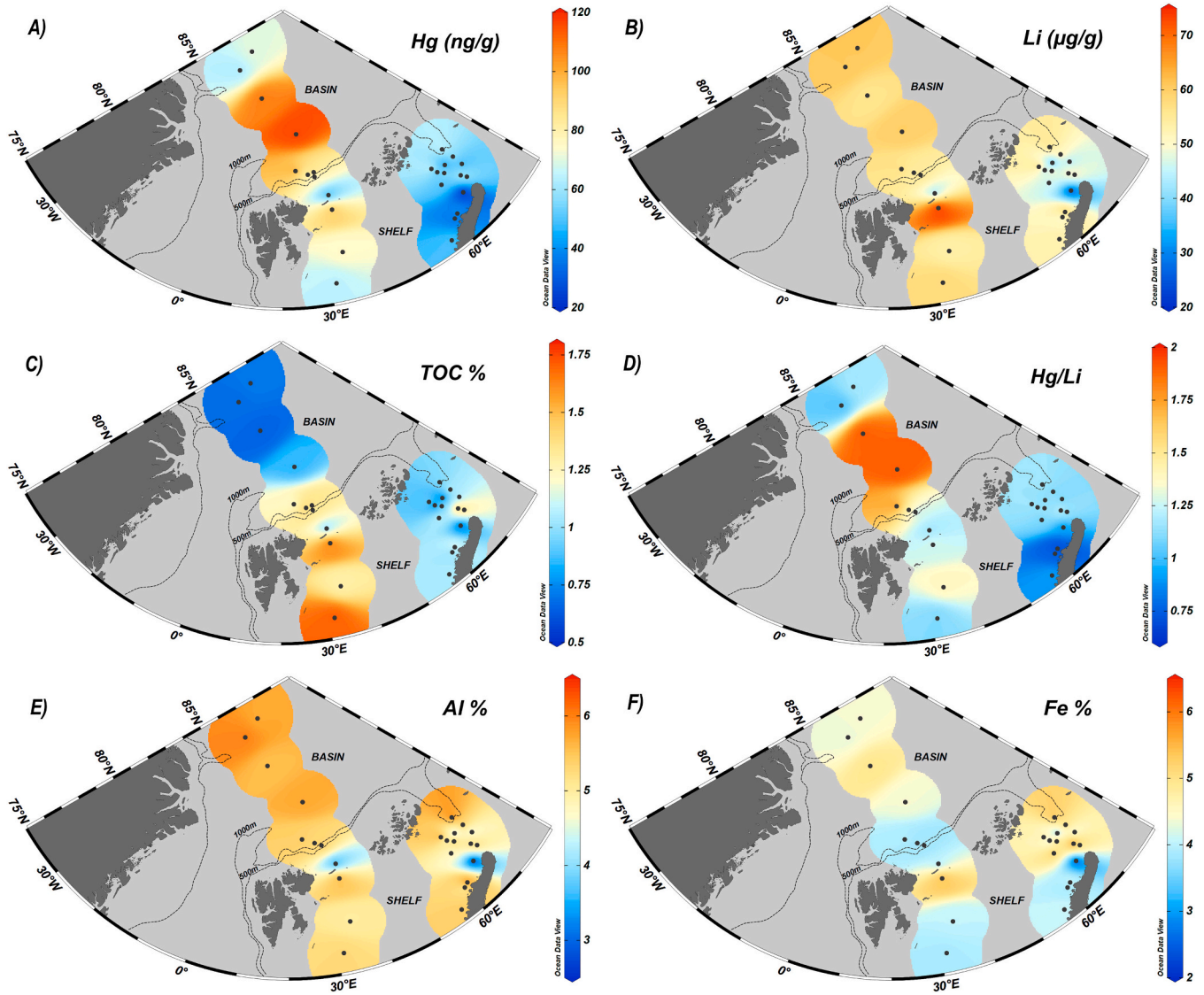

Fig. 2. Distributions of Hg, Li, TOC, Hg/Li, Al, and Fe in surface sediments of the northern Barents Sea and Eurasian Basin. Figure created using Ocean Data View.

reported in the Arctic Basin as well as the surrounding Arctic shelf seas (Table 1). The highest Hg concentrations of 87 ± 20 ng/g (range: 63–116 ng/g, $n = 8$) were observed in the Eurasian Basin (bottom depth > 1000 m), with the maximum Hg values observed in the deepest part of the Nansen Basin at station P8. On the shelf (bottom depth < 542 m), average Hg concentrations were lower at 55 ± 17 ng/g (range: 21–94 ng/g, $n = 18$) with the lowest values observed in the northeastern Barents Sea near Novaya Zemlya. Furthermore, our Hg concentrations suggest an increasing trend northward when compared to bulk Hg concentrations in surface sediments of the southern Barents Sea (Knies et al., 2008).

The TOC % content appears to show the opposite trend to our bulk Hg concentrations, with TOC % content higher on the shelf than in the central basin (Fig. 2C). The lowest values are observed in the northeastern Barents Sea (R15, 0.62 %) and the Eurasian Basin (P9, 0.66 %), while the highest TOC % is observed in the northwestern Barents Sea (P1, 1.71 %). P1 is south of the polar front and impacted by Atlantic Water, with higher primary productivity than the more northward Polar Water stations. Lower TOC concentrations on the shelf (R15, P5) could be associated with localized sand banks and shallower areas. Higher sedimentary TOC concentrations in the northern Barents Sea shelf most likely reflect the higher rates of primary production and 1–2 orders of magnitude difference in vertical particulate organic carbon (POC) export (Reigstad et al., 2008) compared to the central Arctic Basin (Nöthig et al., 2020). However, TOC % contents in the Nansen Basin next to the shelf break and slope (P6, P7.1, P7.2, SICE4) show similar values to shelf stations in the northwestern Barents Sea. Higher TOC % in this area may be due to increased primary productivity and vertical export in the ice-free West Spitsbergen Current which flows along the slope parallel to Svalbard (Loeng, 1991) or settling of OC from advected resuspended sediment (Thomsen et al., 2001). Intrusion of the West Spitsbergen Current could explain the higher TOC concentrations at P4. Overall, our higher TOC % contents in the northern Barents Sea are in line with previous studies in the same area (Carroll et al., 2008; Faust et al., 2020).

Bulk concentrations for trace elements are presented in Fig. 3 and averages in Supplementary Data Table 2. Our bulk trace metal concentrations are similar to previous studies in this region (Faust et al., 2020; Maslov et al., 2020; Novikov, 2017) yet trend slightly higher than the southern Barents Sea (Budko et al., 2022; Knies et al., 2008). Furthermore, our shelf stations are comparable to other trace metal concentrations found in the Laptev and East Siberian Seas (Li et al., 2021; Sattarova et al., 2021) and the Chukchi Sea (Cai et al., 2011; Sattarova et al., 2022; Trefry et al., 2014). Elements Co, Ni, Cu, and Pb exhibited higher concentrations in the deep basin (Fig. 3D, E, F, K), while elements Fe, V, As, and Ag appeared higher on the shelf (Fig. 2F, 3A, H, I). In the basin, high concentrations of Co, Ni, and Cu may reflect the transportation of these metals complexed with dissolved OM within the transpolar drift (Charette et al., 2020) and subsequent scavenging with particulate matter. The highest concentrations of Pb were just off the continental shelf along the slope and into the basin, suggesting rapid scavenging of Pb and/or sediment focusing in this region. Other elements in our study area (Cr, Zn, Cd) exhibited no clear trend with regards to shelf or basin enrichments (Fig. 3B, G, J). In general, bulk Mn concentrations are higher in the Arctic Basin (Ye et al., 2019), although one station on the shelf, P4, had unusually high concentrations of Mn (Fig. 3C). A manganese nodule was found at this station, most likely due to the high sedimentary Mn content in this particular area (Ye et al., 2019), which could indicate an active redox environment and explain elevated levels of V, Ni, Zn, As, and Cd.

We evaluated EFs of toxic elements of concern Cr, Ni, Cu, Zn, As, Cd, Hg and Pb and present average EFs of all stations in Fig. 4. Elements have EFs of 1.4 ± 0.2 (Cr), 1.1 ± 0.2 (Ni), 1.1 ± 0.3 (Cu), 0.9 ± 0.1 (Zn), 3.0 ± 1.7 (As), 0.4 ± 0.2 (Cd), 1.1 ± 0.3 (Hg), and 0.9 ± 0.2 (Pb). Therefore, EFs above natural background levels (> 1.0) could indicate local anthropogenic sources of metals or increased metal concentrations on particles delivered to sediment. The average Hg EF was 1.1 ± 0.3, suggesting relatively uniform increases in Hg accumulation for most stations. Basin stations SICE4, P8, and P9 show the highest Hg EFs between 1.7 and 1.9, which could suggest higher anthropogenic accumulation. Additionally, stations P8 and P9 are close to the Gakkel Ridge which could suggest Hg input from this active fault between the Amundsen and Nansen Basins. Although, this enrichment could also be due to upward diffusion of Hg and re-precipitation in surface sediments due to the combination of redox processes (Gobeil et al., 1999) and low sedimentation rates in the Central Basin, between 0.002 and 0.05 mm/yr (Polyak et al., 2009). The average EF of As (3.0 ± 1.7) suggests potential anthropogenic enrichment, although the elevated surface As concentrations could also indicate an active redox cycle with tight coupling to both Fe and Mn (Herbert et al., 2020). We compared our bulk metal concentrations to the sediment classification guidelines outlined by the Norwegian Environment Agency (Supplementary Data Table 3), which aims to identify the toxicity risk to organisms. Elements Cr, Cu, Zn, Cd, Hg and Pb were attributed to "background" or "low risk" concentrations for all stations while Ni and As for most stations were classified as "moderate" risk. Only a few stations exhibited bulk As values as "high" toxicity risk, suggesting a local source of As, possibly in As-rich rocks along the continental margins of Franz Josef Land and Svalbard (Geissler et al., 2019).

To explore the relationships amongst the various elements, PCA of all measured parameters was performed (Fig. 5). Two PCs were extracted, explaining 66 % of the total variance for surface samples. Most parameters (Al, Fe, Li, V, Cr, Mn, Co, Ni, Cu, Zn, Hg, LOI) had significant positive loadings on PC1 (Supplementary Data Table 4) while Si had a significant negative loading. PC1 explained 48 % of the total variance, and most likely reflects the lithogenic characteristics and local topography of the region. Fine-grained aluminosilicates (<63 μm grain size) of terrigenous origin make up most of the region, with decreasing grain size from the shelf into the basin (Wahsner et al., 1999). Varying topographic conditions on the shelf, such as troughs and sand banks, may also reflect sedimentary trace metal distributions. We suspect that many of our element distributions in the northern Barents Sea are driven by the terrigenous origin of sediments. Therefore, we normalized all parameters from all stations to Li (Fig. 2B) as a proxy for fine grained sediments to account for the natural grain size variability.

Normalized Hg concentrations for all sediment samples show significant positive correlations with typically scavenged metals Mn, Co, Cu, and Pb ($p < 0.05$, Supplementary Data Table 6). Increased concentrations of Co and Cu on slope sediments and into the Arctic Basin (Li et al., 2021) have been attributed to metals sourced from shallower regions that are advected towards the basin (Charette et al., 2020) and scavenged by particulate matter. Furthermore, previous studies have also noted increasing bulk Hg and trace element sediment concentrations along the shelf slope towards the Arctic Basin (Aksentov et al., 2021; Liem-Nguyen et al., 2022; Sattarova et al., 2022). Since this region has no local anthropogenic Hg sources, Hg inputs to sediments are most likely controlled by the scavenging rate of Hg to sinking particles (Hare et al., 2010). If we assume constant sedimentation rates, variations in Hg/Li (Fig. 2D) are due to an increase of Hg on sinking particles and/or an increase in the proportion of particles that can scavenge Hg (Hare et al., 2010). Our high Hg/Li ratios and increased Mn content in the Nansen Basin may reflect sinking particulate matter composition. Indeed, studies have shown both higher particulate Hg concentrations, and greater proportions of Mn oxides, in suspended particulate matter in the Arctic Basin compared to the Arctic shelves (Tesán et al., 2020; Xiang and Lam, 2020). Consequently, we propose that our spatial distributions of Hg in surface sediments reflect hydrodynamic transport of particles and scavenging mechanisms operating in the northern Barents Sea and Eurasian Basin.

In summer, high primary production and particulate OM export plays a major role in scavenging Hg and other metals to deeper waters and sediments. However, Fe and Mn oxides could also scavenge Hg and

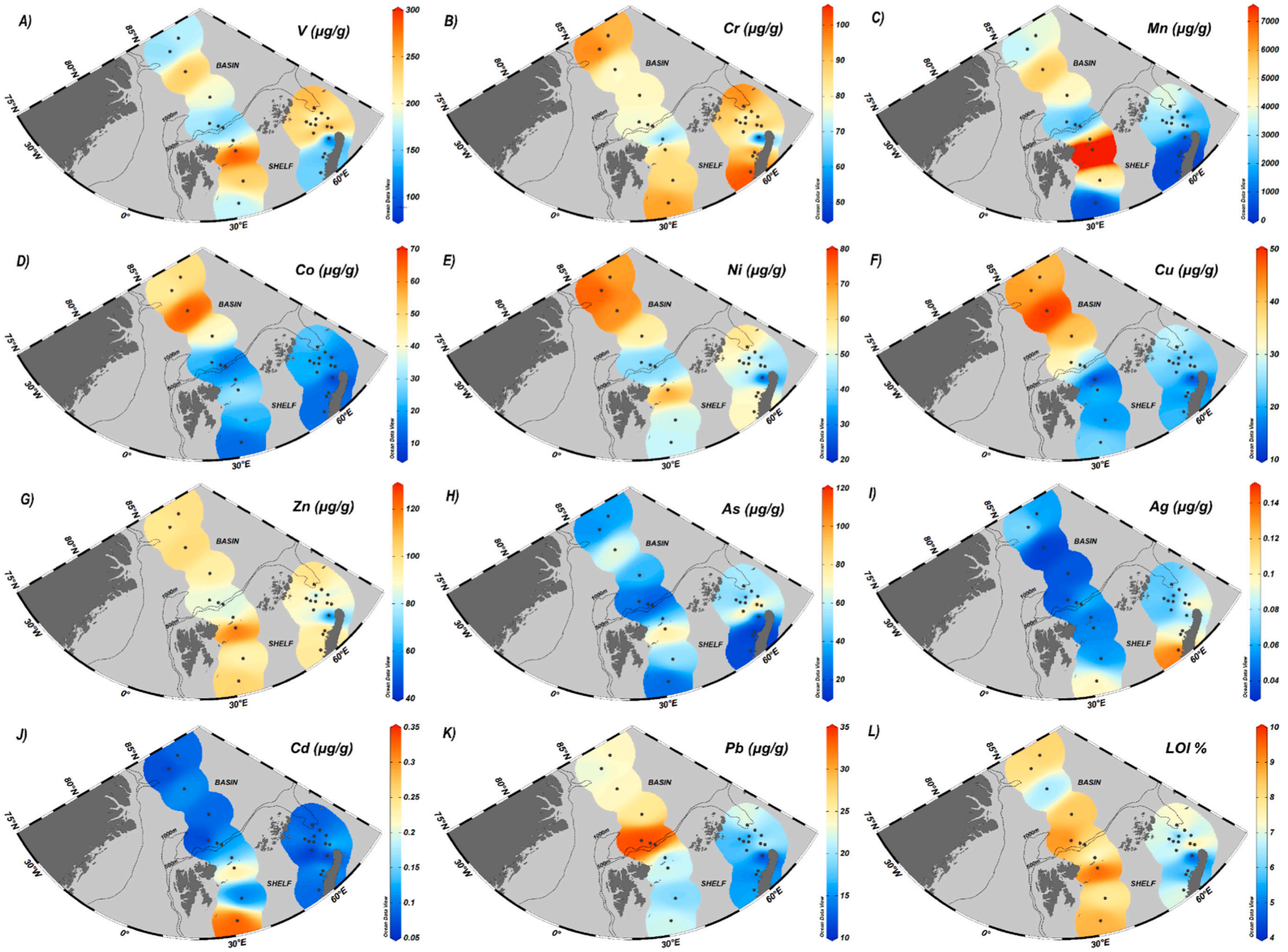

Fig. 3. Distributions of V, Cr, Mn*, Co, Ni, Cu, Zn, As, Ag, Cd, Pb, and LOI in the northern Barents Sea and Arctic Basin. Figure created using Ocean Data View. *Station P4 Mn concentration (13,826 µg/g) is plotted as the maximum range (7500 µg/g).

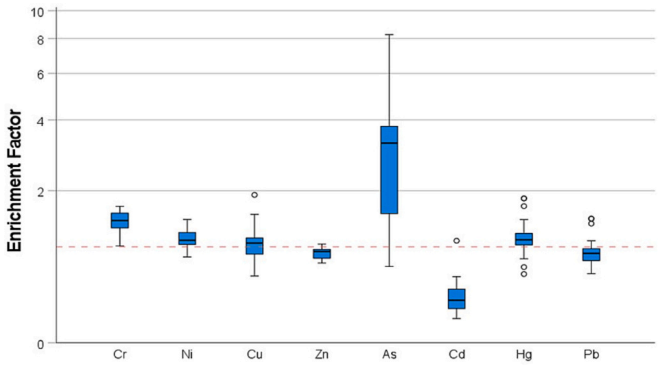

Fig. 4. Average enrichment factors for Cr, Ni, Cu, Zn, As, Cd, Hg and Pb for all sampled stations. The expected natural ratio of 1.0 is marked with a dotted red line. Unfilled circles represent stations identified as numerical outliers using Tukey's method. Note the Y-axis is in a logarithmic scale. (For interpretation of the references to colour in this figure legend, the reader is referred to the web version of this article.)

other particle reactive elements in the Arctic Ocean (Bam et al., 2020; Cui et al., 2021; Lamborg et al., 2016), especially when particulate OM fluxes decline during the Arctic's polar night. Depletion of ^{230}Th, a particle reactive tracer, in waters of the Amundsen Basin has already suggested the presence of intense scavenging over the Barents Sea shelf (Valk et al., 2020). Additionally, recent research has observed that seasonal losses of Hg and Pb in the water column of the Barents Sea may be due to scavenging by Mn oxides (Kohler et al., 2022). High concentrations of dissolved Mn^{2+} in the water column of the Barents Sea (Kohler et al., 2022; Middag et al., 2011) are most likely released from benthic sources during winter overturning after high inputs of seasonal OM (Macdonald and Gobeil, 2012; Vieira et al., 2019). Winter mixing and storms resuspend Mn into winter sea ice which can drift into the basins (Rogalla et al., 2022). In addition, this turbulence generates a nepheloid layer rich in suspended sediment in shallow Barents Sea bottom waters (Gardner et al., 2022). These particles are advected and entrained within sinking dense water plumes into the Nansen Basin (Rudels et al., 2000), as evidenced by deep water measurements of dissolved Al, Fe, and Ba (Klunder et al., 2012; Middag et al., 2009; Roeske et al., 2012). Simultaneously, these hydrodynamic processes may deliver Hg and other metals towards the Eurasian Basin, where the oxidation of Mn during the polar night (Xiang et al., 2021) scavenges Hg and particle reactive metals to sediments. As a result, these processes may help explain our higher sedimentary concentrations of Hg, Co, Cu, and Pb in the Eurasian Basin. We hypothesize that the entire Arctic Basin contains some similarities to deep trench environments, where sediment focusing concentrates Hg and other metals sourced from shallower areas (Sanei et al., 2021). In addition, we speculate that similar transport processes and subsequent particle scavenging also influence Hg sediment distributions on the other Arctic shelves.

PC2 (Fig. 5) explains about 19 % of the variance with significant positive loadings for Ag, Cd, and TOC % and negative loadings for Mn, Co, Cu, and Hg. This component is most likely related to depth or geographic region, as negative loadings for Mn, Co, Cu, and Hg reflect higher bulk concentrations in the basin compared to concentrations on the shelf. As a result, PC2 further supports a Mn scavenging transport

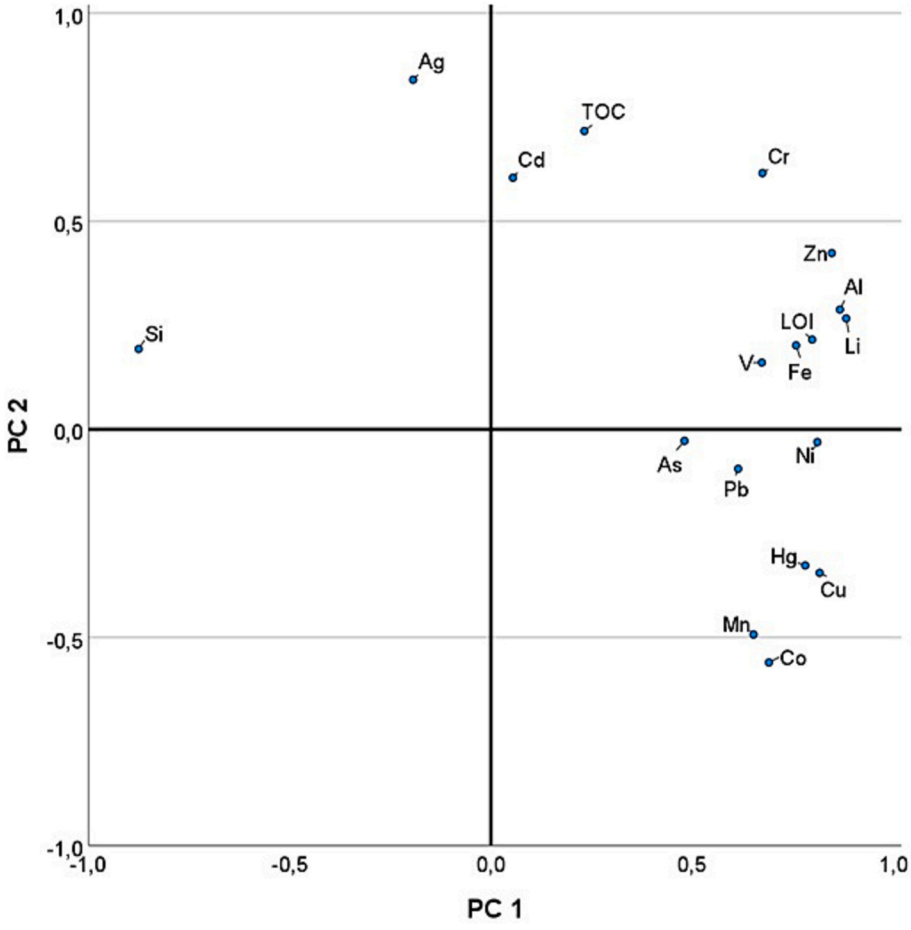

Fig. 5. Rotated factor loadings for two principal components ($n = 24$) for all measured parameters and Si*. P4 excluded for Mn outlier (Supplementary Data Fig. 2). *Si measurement details in Supplementary Data.

mechanism operating into the Eurasian Basin. The significant positive loading of Ag on PC2 could be explained by higher Ag concentrations in the northeastern Barents Sea due to terrestrial runoff from Ag-bearing ores and anthropogenic mining activity located on Novaya Zemyla (Korago et al., 2022). The positive loadings for TOC and Cd however, most likely reflect higher primary productivity and POC fluxes in the marginal ice zone, with possible Cd uptake as a micronutrient into sinking diatoms (Morel et al., 2020). Phytoplankton Cd uptake, sinking, and sediment burial is further supported by a positive correlation between TOC % and Cd (Supplementary Data Table 6). Due to high primary productivity and vertical POC export on the shelf, we expect sedimentary trace metal distributions to reflect phytoplankton uptake, adsorption and scavenging of Hg and other micronutrients. However, a Pearson correlation table for normalized shelf concentrations only, indicates that TOC shows no significant positive correlations with any other elements except Cd (Supplementary Data Table 7). This lack of correlation suggests that Hg and trace elements may be delivered to sediments via adsorption to different types of particles other than POC or that active sedimentary diagenetic processes distort the expected OC-metal relationship. We did find that many elements (V, Cr, Co, Ni, Cu, Zn, As, Pb) show significant positive correlations to Fe (Supplementary Data Table 7). This finding is supported by the importance of Fe as an anaerobic carbon mineralization pathway in Barents Sea sediments (Vandieken et al., 2006). After oxygen, OC derived from marine sources (Faust et al., 2020) is remineralized in the sediment using Fe and Mn as terminal electron acceptors. Upwards diffusion and coprecipitation of authigenic Fe and Mn at the sediment-water interface adsorbs trace elements. This active redox environment may also explain Hg's significant positive correlation with Mn, V, and As on the Barents Sea shelf (Supplementary Data Table 7). As mentioned previously, winter mixing may resuspend both reduced Fe and Mn into the water column, leading to increased scavenging on the shelf.

In this study, we investigated the spatial distribution of Hg in surface sediments in the northern Barents Sea and Eurasian Basin. Bulk concentrations of Hg and trace elements in these areas are comparable to other areas of the Arctic Ocean. Calculated EF values for Hg and elements of concern indicate low anthropogenic influence and suggest a low toxicity risk according to the Norwegian Environment Agency. The distribution of Hg and trace elements are most likely driven by the transport of fine grain sediment, scavenging by both particulate OM and Fe/Mn oxides, and active sedimentary redox processes. Our observations establish a baseline of Hg and trace metals in the northern Barents Sea and Eurasian Basin that can be used for models, budgets, and ecological assessments in an era of rapid Arctic change.

CRediT authorship contribution statement

Stephen G. Kohler: Conceptualization, methodology, validation, formal analysis, investigation, writing - original draft, visualization. **Laura M. Kull**: Methodology, validation, formal analysis, investigation, writing - review and editing, visualization. **Lars-Eric Heimbürger-Boavida:** Writing - review and editing, supervision. **Thaise Ricardo de Freitas:** Formal analysis, writing - review and editing. **Nicolas Sanchez:** Writing - review and editing. **Kuria Ndungu:** Writing - review and editing, supervision. **Murat V. Ardelan:** Conceptualization, resources, writing - review and editing, supervision, funding acquisition.

Declaration of competing interest

The authors declare no competing interests.

Data availability

Data will be made available on request.

Acknowledgments

The authors are grateful to the captain, crew, cruise leaders, and fellow scientists onboard R/V *Kronprins Haakon* on cruises Q3, Q4, Q1, Q2, and JC2-2, as part of the Nansen Legacy Project (RCN#276730). In particular, the authors wish to thank the Benthos teams (B. Bluhm, T. Ciesielski, S. Hess, E. Jordà Molina, C. Lockwood-Ireland, B. Schuppe, A. Sen, A. Ziegler) on each cruise for help in collecting the samples. The authors would also like to thank the captain, crew, and scientists involved (A. Bambulyak, A. Deryabin, D. Moiseev, V. Savinov) with the R/V *Dalniye Zelentsy* expedition from the Murmansk Marine Biological Institute (MMBI) for help in collecting and transporting the samples from the northeastern Barents Sea. Additional thanks are to A. Simić, K. Seyitmuhammedov, and Ø. Mikkelsen for help with parts of the analyses.

Appendix A. Supplementary data

Supplementary data to this article can be found online at https://doi.org/10.1016/j.marpolbul.2022.114272.

References

Abrahim, G.M., Parker, R.J., 2008. Assessment of heavy metal enrichment factors and the degree of contamination in marine sediments from Tamaki Estuary, Auckland, New Zealand. Environ. Monit. Assess. 136, 227–238. https://doi.org/10.1007/s10661-007-9678-2.

Aksentov, K.I., et al., 2021. Assessment of mercury levels in modern sediments of the east Siberian Sea. Mar. Pollut. Bull. 168, 112426 https://doi.org/10.1016/j.marpolbul.2021.112426.

Asmund, G., Nielsen, S.P., 2000. Mercury in dated Greenland marine sediments. Sci. Total Environ. 245, 61–72. https://doi.org/10.1016/s0048-9697(99)00433-7.

Bam, W., et al., 2020. Variability in 210Pb and 210Po partition coefficients (Kd) along the US GEOTRACES Arctic transect. Mar. Chem. 219, 103749 https://doi.org/10.1016/j.marchem.2020.103749.

Budko, D.F., Demina, L.L., Travkina, A.V., Starodymova, D.P., Alekseeva, T.N., 2022. The features of distribution of chemical elements, including heavy metals and Cs-137, in surface sediments of the Barents, Kara, Laptev and East Siberian Seas. Minerals 12, 328. https://doi.org/10.3390/min12030328.

Cai, M.H., Lin, J., Hong, Q.Q., Wang, Y., Cai, M.G., 2011. Content and distribution of trace metals in surface sediments from the northern Bering Sea, Chukchi Sea and adjacent Arctic areas. Mar. Pollut. Bull. 63, 523–527. https://doi.org/10.1016/j.marpolbul.2011.02.007.

Carroll, J., et al., 2008. Accumulation of organic carbon in western Barents Sea sediments. Deep-Sea Res. II Top. Stud. Oceanogr. 55, 2361–2371. https://doi.org/10.1016/j.dsr2.2008.05.005.

Charette, M.A., et al., 2020. The transpolar drift as a source of riverine and shelf-derived trace elements to the Central Arctic Ocean. J. Geophys. Res. Oceans 125, e2019JC015920. https://doi.org/10.1029/2019JC015920.

Chetélat, J., et al., 2022. Climate change and mercury in the Arctic: abiotic interactions. Sci. Total Environ. 824, 153715 https://doi.org/10.1016/j.scitotenv.2022.153715.

Cui, X., Lamborg, C.H., Hammerschmidt, C.R., Xiang, Y., Lam, P.J., 2021. The effect of particle composition and concentration on the partitioning coefficient for mercury in three ocean basins. Front. Environ. Chem. 2, 660267 https://doi.org/10.3389/fenvc.2021.660267.

Dastoor, A., et al., 2022. Arctic mercury cycling. Nat. Rev. Earth Environ. https://doi.org/10.1038/s43017-022-00269-w.

Everaert, G., et al., 2017. Additive models reveal sources of metals and organic pollutants in Norwegian marine sediments. Environ. Sci. Technol. 51, 12764–12773. https://doi.org/10.1021/acs.est.7b02964.

Faust, J.C., et al., 2020. Does Arctic warming reduce preservation of organic matter in Barents Sea sediments? Philos. Transact. A Math. Phys. Eng. Sci. 378, 20190364 https://doi.org/10.1098/rsta.2019.0364.

Fox, A.L., et al., 2014. Mercury in the northeastern Chukchi Sea: distribution patterns in seawater and sediments and biomagnification in the benthic food web. Deep-Sea Res. II Top. Stud. Oceanogr. 102, 56–67. https://doi.org/10.1016/j.dsr2.2013.07.012.

Gardner, W.D., Richardson, M.J., Mishonov, A.V., Lam, P.J., Xiang, Y., 2022. Distribution, sources, and dynamics of particulate matter along trans-arctic sections. J. Geophys. Res. Oceans 127, e2021JC017970. https://doi.org/10.1029/2021JC017970.

Geissler, W.H., et al., 2019. Middle Miocene magmatic activity in the Sophia Basin, Arctic Ocean—evidence from dredged basalt at the flanks of Mosby Seamount. Arktos 5, 31–48. https://doi.org/10.1007/s41063-019-00066-8.

Gobeil, C., Macdonald, R.W., Smith, J.N., 1999. Mercury profiles in sediments of the Arctic Ocean basins. Environ. Sci. Technol. 33, 4194–4198. https://doi.org/10.1021/es990471p.

Hare, A.A., et al., 2010. Natural and anthropogenic mercury distribution in marine sediments from Hudson Bay, Canada. Environ. Sci. Technol. 44, 5805–5811. https://doi.org/10.1021/es100724y.
Heiri, O., Lotter, A.F., Lemcke, G., 2001. Loss on ignition as a method for estimating organic and carbonate content in sediments: reproducibility and comparability of results. J. Paleolimnol. 25, 101–110. https://doi.org/10.1023/A:1008119611481.
Herbert, L.C., et al., 2020. Glacial controls on redox-sensitive trace element cycling in Arctic fjord sediments (Spitsbergen, Svalbard). Geochim. Cosmochim. Acta 271, 33–60. https://doi.org/10.1016/j.gca.2019.12.005.
[dataset] Jensen, H., Knies, J., Boitsov, S., 2022. Database for composition of marine sediments, [MAREANO]. Updated 04-01. Geological Survey of Norway (NGU). https://mareano.no/en/maps-and-data/chemical-data.
Kim, J., et al., 2020. Mass budget of methylmercury in the east Siberian Sea: the importance of sediment sources. Environ. Sci. Technol. 54, 9949–9957. https://doi.org/10.1021/acs.est.0c00154.
Klunder, M.B., Laan, P., Middag, R., de Baar, H.J.W., Bakker, K., 2012. Dissolved iron in the Arctic Ocean: important role of hydrothermal sources, shelf input and scavenging removal. J. Geophys. Res. Oceans 117, C04014. https://doi.org/10.1029/2011JC007135.
Knies, J., Jensen, H., Finne, T., Lepland, A., Sæther, O., 2008. In: Sediment Composition and Heavy Metal Distribution in Barents Sea Surface Samples: Results From Institute of Marine Research 2003 and 2004 cruises. NGU report, pp. 1–44.
Kohler, S.G., et al., 2022. Arctic Ocean's wintertime mercury concentrations limited by seasonal loss on the shelf. Nat. Geosci. 15, 621–626. https://doi.org/10.1038/s41561-022-00986-3.
Korago, E.A., et al., 2022. Geological structure of the Novaya Zemlya archipelago (West russian Arctic) and peculiarities of the tectonics of the eurasian Arctic. Geotectonics 56, 123–156. https://doi.org/10.1134/S0016852122020030.
Lamborg, C.H., Hammerschmidt, C.R., Bowman, K.L., 2016. An examination of the role of particles in oceanic mercury cycling. Philos. Transact. A Math. Phys. Eng. Sci. 374, 20150297 https://doi.org/10.1098/rsta.2015.0297.
Lee, J.H., et al., 2021. Climate-associated changes in mercury sources in the Arctic Fjord sediments. ACS Earth Space Chem. 5, 2398–2407. https://doi.org/10.1021/acsearthspacechem.1c00095.
Li, L., et al., 2021. Enrichment of trace metals (V, cu co, ni, and Mo) in Arctic sediments-from Siberian Arctic shelves to the basin. J. Geophys. Res. Oceans 126, e2020JC016960. https://doi.org/10.1029/2020JC016960.
Liem-Nguyen, V., et al., 2022. Spatial patterns and distributional controls of total and methylated mercury off the Lena River in the Laptev Sea sediments. Mar. Chem. 238, 104052 https://doi.org/10.1016/j.marchem.2021.104052.
Lind, S., Ingvaldsen, R.B., Furevik, T., 2018. Arctic warming hotspot in the northern Barents Sea linked to declining sea-ice import. Nat. Clim. Chang. 8, 634–639. https://doi.org/10.1038/s41558-018-0205-y.
Loeng, H., 1991. Features of the physical oceanographic conditions of the Barents Sea. Polar Res. 10, 5–18. https://doi.org/10.1111/j.1751-8369.1991.tb00630.x.
Loring, D.H., 1990. Lithium - a new approach for the granulometric normalization of trace-metal data. Mar. Chem. 29, 155–168. https://doi.org/10.1016/0304-4203(90)90011-Z.
Macdonald, R.W., Gobeil, C., 2012. Manganese sources and sinks in the Arctic Ocean with reference to periodic enrichments in basin sediments. Aquat. Geochem. 18, 565–591. https://doi.org/10.1007/s10498-011-9149-9.
Maslov, A.V., Politova, N.V., Kozina, N.V., Shevchenko, V.P., Alekseeva, T.N., 2020. Rare and trace elements in the modern bottom sediments of the Barents Sea. Lithol. Miner. Resour. 55, 1–23. https://doi.org/10.1134/S0024490220010058.
Mazrui, N.M., Jonsson, S., Thota, S., Zhao, J., Mason, R.P., 2016. Enhanced availability of mercury bound to dissolved organic matter for methylation in marine sediments. Geochim. Cosmochim. Acta 194, 153–162. https://doi.org/10.1016/j.gca.2016.08.019.
McKinney, M.A., et al., 2022. Climate change and mercury in the Arctic: biotic interactions. Sci. Total Environ. 834, 155221 https://doi.org/10.1016/j.scitotenv.2022.155221.
Middag, R., de Baar, H.J.W., Laan, P., Bakker, K., 2009. Dissolved aluminium and the silicon cycle in the Arctic Ocean. Mar. Chem. 115, 176–195. https://doi.org/10.1016/j.marchem.2009.08.002.
Middag, R., de Baar, H.J.W., Laan, P., Klunder, M.B., 2011. Fluvial and hydrothermal input of manganese into the Arctic Ocean. Geochim. Cosmochim. Acta 75, 2393–2408. https://doi.org/10.1016/j.gca.2011.02.011.
Morel, F.M.M., Lam, P.J., Saito, M.A., 2020. Trace metal substitution in marine phytoplankton. Annu. Rev. Earth Planet. Sci. 48, 491–517. https://doi.org/10.1146/annurev-earth-053018-060108.
Nöthig, E.M., et al., 2020. Annual cycle of downward particle fluxes on each side of the Gakkel ridge in the Central Arctic Ocean. Philos. Transact. A Math. Phys. Eng. Sci. 378, 20190368 https://doi.org/10.1098/rsta.2019.0368.
Novikov, M., 2017. On the background values of heavy metal content in bottom sediments of the Barents Sea. Bull. Murmansk State Tech. Univ. 20, 280–288. https://doi.org/10.21443/1560-9278-2017-20-1/2-280-288.
Polyak, L., et al., 2009. Late quaternary stratigraphy and sedimentation patterns in the western Arctic Ocean. Glob. Planet. Chang. 68, 5–17. https://doi.org/10.1016/j.gloplacha.2009.03.014.
Reigstad, M., Riser, C.W., Wassmann, P., Ratkova, T., 2008. Vertical export of particulate organic carbon: attenuation, composition and loss rates in the northern Barents Sea. Deep-Sea Res. II Top. Stud. Oceanogr. 55, 2308–2319. https://doi.org/10.1016/j.dsr2.2008.05.007.
Roeske, T., van der Loeff, M.R., Middag, R., Bakker, K., 2012. Deep water circulation and composition in the Arctic Ocean by dissolved barium, aluminium and silicate. Mar. Chem. 132, 56–67. https://doi.org/10.1016/j.marchem.2012.02.001.
Rogalla, B., Allen, S.E., Colombo, M., Myers, P.G., Orians, K.J., 2022. Sediments in sea ice drive the Canada Basin surface mn maximum: insights from an Arctic Mn Ocean model. Glob. Biogeochem. Cycles 36, e2022GB007320. https://doi.org/10.1029/2022gb007320.
Rudels, B., Muench, R.D., Gunn, J., Schauer, U., Friedrich, H.J., 2000. Evolution of the Arctic Ocean boundary current north of the siberian shelves. J. Mar. Syst. 25, 77–99. https://doi.org/10.1016/S0924-7963(00)00009-9.
Sanei, H., et al., 2021. High mercury accumulation in deep-ocean hadal sediments. Sci. Rep. 11, 10970. https://doi.org/10.1038/s41598-021-90459-1.
Sattarova, V., et al., 2021. Trace metals in surface sediments from the laptev and east siberian seas: levels, enrichment, contamination assessment, and sources. Mar. Pollut. Bull. 173, 112997 https://doi.org/10.1016/j.marpolbul.2021.112997.
Sattarova, V., et al., 2022. Distribution and assessment of trace metals in modern bottom sediments in the southwestern Chukchi Sea. Mar. Pollut. Bull. 180, 113797 https://doi.org/10.1016/j.marpolbul.2022.113797.
Schlitzer, R., 2021. Ocean Data View, odv.awi.de.
Schuster, P.F., et al., 2018. Permafrost stores a globally significant amount of mercury. Geophys. Res. Lett. 45, 1463–1471. https://doi.org/10.1002/2017gl075571.
Tesán, J., et al., 2020. Mercury export flux in the Arctic Ocean estimated from 234Th: 238U disequilibria. ACS Earth Space Chem. 4, 795–801. https://doi.org/10.1021/acsearthspacechem.0c00055.
Thomsen, C., Blaume, F., Fohrmann, H., Peeken, I., Zeller, U., 2001. Particle transport processes at slope environments - event driven flux across the Barents Sea continental margin. Mar. Geol. 175, 237–250. https://doi.org/10.1016/S0025-3227(01)00143-8.
Trefry, J.H., Trocine, R.P., Cooper, L.W., Dunton, K.H., 2014. Trace metals and organic carbon in sediments of the northeastern Chukchi Sea. Deep-Sea Res. II Top. Stud. Oceanogr. 102, 18–31. https://doi.org/10.1016/j.dsr2.2013.07.018.
Valk, O., et al., 2020. Decrease in 230Th in the Amundsen Basin since 2007: far-field effect of increased scavenging on the shelf? Ocean Sci. 16, 221–234. https://doi.org/10.5194/os-16-221-2020.
Vandieken, V., Nickel, M., Jorgensen, B.B., 2006. Carbon mineralization in Arctic sediments northeast of Svalbard: Mn(IV) and Fe(III) reduction as principal anaerobic respiratory pathways. Mar. Ecol. Prog. Ser. 322, 15–27. https://doi.org/10.3354/meps322015.
Vieira, L.H., et al., 2019. Benthic fluxes of trace metals in the Chukchi Sea and their transport into the Arctic Ocean. Mar. Chem. 208, 43–55. https://doi.org/10.1016/j.marchem.2018.11.001.
Wahsner, M., et al., 1999. Clay-mineral distribution in surface sediments of the eurasian Arctic Ocean and continental margin as indicator for source areas and transport pathways - a synthesis. Boreas 28, 215–233. https://doi.org/10.1111/j.1502-3885.1999.tb00216.x.
Xiang, Y., Lam, P.J., 2020. Size-fractionated compositions of marine suspended particles in the Western Arctic Ocean: lateral and vertical sources. J. Geophys. Res. Oceans 125, e2020JC016144. https://doi.org/10.1029/2020JC016144.
Xiang, Y., Lam, P.J., Lee, J.M., 2021. Diel redox cycle of manganese in the surface Arctic Ocean. Geophys. Res. Lett. 48, e2021GL094805 https://doi.org/10.1029/2021GL094805.
Ye, L., März, C., Polyak, L., Yu, X., Zhang, W., 2019. Dynamics of manganese and cerium enrichments in Arctic Ocean sediments: a case study from the alpha ridge. Front. Earth Sci. 6 https://doi.org/10.3389/feart.2018.00236.
Zaborska, A., et al., 2008. Recent sediment accumulation rates for the Western margin of the Barents Sea. Deep-Sea Res. II Top. Stud. Oceanogr. 55, 2352–2360. https://doi.org/10.1016/j.dsr2.2008.05.026.